Control of sporulation-specific cell division in Streptomyces coelicolor

Noens, E.

2

SsgA-like proteins determine the fate of peptidoglycan during sporulation of *Streptomyces coelicolor*

Elke E. E. Noens, Vassilis Mersinias, Bjørn A. Traag,
Colin P. Smith, Henk K. Koerten and Gilles P. van Wezel

Mol Microbiol (2005) 58: 929-944

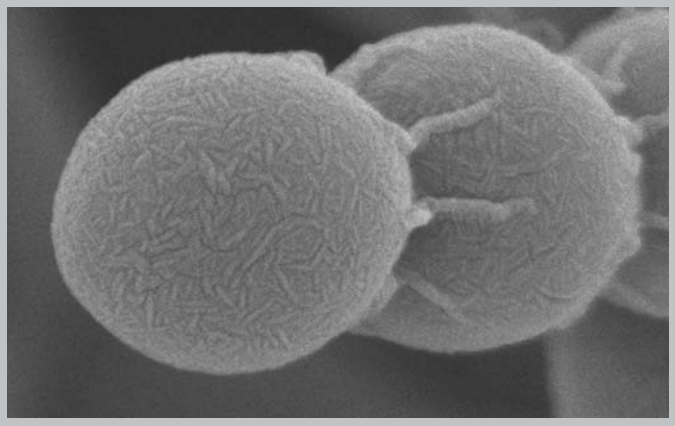

ABSTRACT

During developmental cell division in sporulation-committed aerial hyphae of streptomycetes, up to a hundred septa are simultaneously produced, in close harmony with synchromous chromosome condensation and segregation. Several unique protein families are involved in the control of this process in actinomycetes, including that of the SsgA-like proteins (SALPs). Mutants for each of the individual SALP genes were obtained, and high resolution and fluorescence imaging revealed that each plays an important and highly specific role in the control of the sporulation process, and their function relates to the build-up and degradation of septal and spore-wall peptidoglycan. While SsgA and SsgB are essential for sporulation-specific cell division in *S. coelicolor*, SsgC-G are responsible for correct DNA segregation/condensation (SsgC), spore wall synthesis (SsgD), autolytic spore separation (SsgE, SsgF), or exact septum localisation (SsgG). Our experiments paint a picture of a novel protein family that acts through timing and localisation of the activity of PBPs and autolysins, thus controlling important steps during the initiation and the completion of sporulation in actinomycetes.

INTRODUCTION

Cell division is a highly dynamic process of cell wall synthesis and breakdown, and its correct timing and localisation is one of the most studied topics in modern microbial cell biology. In *E. coli*, such control mechanisms include localisation of the septal ring exactly at the mid-cell position, mediated through the *minCDE* and *sulA* SOS systems (Autret and Errington, 2001; Justice *et al.*, 2000), coordinated peptidoglycan synthesis by penicillin-binding proteins (PBPs; reviewed in (Errington *et al.*, 2003; Holtje, 1998)), and timely DNA duplication and segregation (Errington, 2001; Sharpe and Errington, 1999). While in most bacteria a single septum is formed, that forms the cleavage furrow dividing the mother cell into the daugther cells, during sporulation of the Gram-positive mycelial bacterium *Streptomyces* many septa are simultaneously produced to form long chains of spores. In fact, *Streptomyces* undergoes two apparently different cell division events (Flärdh *et al.*, 2000; McCormick *et al.*, 1994). *Streptomyces* growth on solid media starts with the germination of a single spore that develops into a complex vegetative mycelium of branching hyphae (Chater and Losick, 1997). These vegetative hyphae are divided into connected multinucleoid compartments by vegetative septa or cross-walls. Environmental signals such as nutrient depletion result in the development of initially aseptate aerial hyphae while part of the vegetative mycelium lyses. Eventually, the aerial hyphae are dissected into spores by specialised sporulation septa, producing chains of connected uninucleoid spores (Chater, 2001), which are subsequently separated by a poorly understood process of autolytic cleavage, to produce mature spores. In contrast to cross-walls, sporulation septa are produced simultaneously and in a highly coordinated way. Another important difference with the generally accepted view of microbial cell division is the apparent lack of relatives of FtsA and ZipA, which anchor the spiral ring to the membrane (Errington *et al.*, 2003), and of homologues of *minC, minE,* and *sulA*. Therefore, the hunt is on for the discovery of novel proteins that facilitate the complex mechanism of cell division in *Streptomyces*.

The most well-known group of developmental genes is that of the *whi* genes, which were discovered by their ability to complement the White phenotype of non-sporulating and/or non-pigmented aerial hyphae (Chater, 1972; Chater, 1998). In more recent years, several important new families of developmental proteins were discovered, including the rodlins ((Claessen *et al.*, 2002)) and chaplins (Claessen *et al.*, 2003; Elliot *et al.*, 2003), hydrophobins and hydrophobin-like proteins respectively providing a water-repellant sheath

around the aerial hyphae, and the WhiB-like (Wbl) proteins, a family of small regulatory proteins with diverse targets that are also found in non-sporulating actinomycetes such as *Mycobacterium* (Soliveri *et al.*, 2000).

An emerging group of novel developmental regulators is that of the SsgA-like proteins (SALPs), which occur exclusively in sporulating actinomycetes (reviewed in (van Wezel and Vijgenboom, 2004)). Seven homologues occur in *S. coelicolor* (designated SsgA-G), and six in *S. avermitilis* ((van Wezel and Vijgenboom, 2004)). All SALPs are relatively small (125-142 aa) proteins ((Keijser *et al.*, 2003)), sharing an average amino acid similarity of 30-40%. The two members that have been studied so far, SsgA and SsgB, are essential for sporulation. The best-studied example is SsgA, which was originally identified as an effecter of cell division in *S. griseus* ((Kawamoto and Ensign, 1995), and specifically stimulates sporulation-specific cell division (van Wezel *et al.*, 2000). *ssgA* null mutants show strongly reduced sporulation, although some viable spores are produced on mannitol-containing media (Jiang and Kendrick, 2000; van Wezel *et al.*, 2000). The different timing and expression of *ssgA* explains some of the major differences in developmental control between the phylogenetically divergent species *S. coelicolor* and *S. griseus*, such as the ability of the latter strain to produce submerged spores, and the more dominant developmental role of γ-butyrolactones in this organism (Traag *et al.*, 2004; Yamazaki *et al.*, 2003). Mutation of *ssgB* resulted in a non-sporulating phenotype under all conditions, producing very large white colonies (Keijser *et al.*, 2003; Kormanec and Sevcikova, 2002)

The non-sporulating phenotypes of the *ssgA* and *ssgB* null mutants, and the fact that they occur exclusively in sporulating actinomycetes, suggested a role for the SALPs specifically during sporulation. We addressed this issue by the creation and intensive study of knock-out mutants of all *ssgA*-like genes of *S. coelicolor*, showing that each SALP is involved in a specific step in the sporulation process, from septum-site selection to the ultimate stages of spore maturation. A working model as to when and how these proteins carry out their function is proposed.

MATERIALS AND METHODS

Bacterial strains and media

The bacterial strains described in this work are listed in Table 1. *E. coli* K-12 strains JM109 (Sambrook *et al.*, 1989) and ET12567 (MacNeil *et al.*, 1992) were used for plasmid propagation, and were grown and transformed by standard procedures (Sambrook *et al.*, 1989). *E. coli* BW25113 (Datsenko and Wanner, 2000) was used to create and propagate the *S. coelicolor* cosmids used for the creation of knock-out mutants of *S. coelicolor* M145. *E. coli* ET12567 containing pUZ8002 was used for conjugation to *S. coelicolor* using the procedure described by Flett *et al*., (1997). Transformants were selected in L broth containing the appropriate antibiotics.

S. coelicolor A3(2) M145 was obtained from the John Innes Centre strain collection, and was the parent for the previously created *ssgA* mutant GSA3 (van Wezel *et al.*, 2000) and *ssgB* mutant GSB1 (Keijser *et al.*, 2003), and for the *ssgC-G* mutants described in this paper. All media and routine *Streptomyces* techniques are described in the *Streptomyces* manual (Kieser *et al.*, 2000). Soy Flour Mannitol (SFM) medium was used for making spore suspensions and R2YE agar plates for regeneration of protoplasts and, after the addition of the appropriate antibiotic, for selecting recombinants. Phenotypic characterisation of mutants was done on SFM, on R2YE (not shown) and on minimal medium agar plates (not shown) with glucose (MMgluc) or mannitol (MMman) as the sole carbon source (Kieser *et al.*, 2000).

Table 1: Bacterial strains.

Bacterial strain	Genotype	Reference
S. coelicolor A3(2)	$SCP1^+$ $SCP2^+$	(Kieser *et al.*, 2000)
S. coelicolor A3(2) M145	$SCP1^-$ $SCP2^-$	(Kieser *et al.*, 2000)
S. coelicolor A3(2) MT1110	$SCP1^-$ $SCP2^-$	(Kieser *et al.*, 2000)
GSA3	M145 Δ*ssgA* (::*aadA*)	(van Wezel *et al.*, 2000)
GSB1	M145 Δ*ssgB* (::*aac(3)IV*)	(Keijser *et al.*, 2003)
GSC1	M145 Δ*ssgC* (::*aac(3)IV*)	This chapter
GSD1	M145 Δ*ssgD* (::*aac(3)IV*)	This chapter
GSE1	M145 Δ*ssgE* (::*aac(3)IV*)	This chapter
GSF1	M145 Δ*ssgF* (::*aac(3)IV*)	This chapter
GSG1	M145 Δ*ssgG* (::*aac(3)IV*)	This chapter
E. coli JM109	See reference	(Sambrook *et al.*, 1989)
E. coli ET12567	See reference	(MacNeil *et al.*, 1992)
E. coli BW25311	See reference	(Gust *et al.*, 2003)
E. coli ET 12567/pUZ8002	See reference	(Gust *et al.*, 2003)

Plasmids, constructs and oligonucleotides

All plasmids and constructs are summarised in Table 2. Required PCRs were done with *Pfu* polymerase (Stratagene), in the presence of 10% (v/v) DMSO, with an annealing temperature of 58^0C. The oligonucleotides are listed in Table S1 (Noens *et al.*, 2005).

Table 2: Plasmids and constructs.

Plasmid/ Cosmid	Description	Reference
pHJL401	*Streptomyces/E. coli* shuttle vector (5-10 and around 100 copies per genome, respectively)	(Larson and Hershberger, 1986)
pIJ2925	Derivative of pUC19 (high copy number) with *Bgl*II sites flanking its multiple cloning site	(Janssen and Bibb, 1993)
pBR322	*E. coli* plasmid with *E. coli* ori (around 50 copies per chromosome)	(Covarrubias *et al.*, 1981)
pBR-KO	Derivative of pBR322 with engineered multiple cloning site and *tsr* gene	(Keijser *et al.*, 2003)
5F2A	Cosmid clone containing *ssgD*	(Bentley *et al.*, 2002)
E87	Cosmid clone containing *ssgE*	(Bentley *et al.*, 2002)
8A11	Cosmid clone containing *ssgF*	(Bentley *et al.*, 2002)
E19A	Cosmid clone containing *ssgG*	(Bentley *et al.*, 2002)
pGWS112	pHJL401 with 1.8 kb fragment harbouring *ssgC* (-1075/+894, relative to *ssgC*)	This chapter
pGWS122	pHJL401 with 900 bp fragment harbouring *ssgD* (-291/+608, relative to *ssgD*)	This chapter
pGWS108	pHJL401 with 1.8 kb fragment harbouring *ssgE* (-732/+1027, relative to *ssgE*)	This chapter
pGWS119	pHJL401 with 1 kb fragment harbouring *ssgF* (-404/+595, relative to *ssgF*)	This chapter
pGWS121	pHJL401 with 1.2 kb fragment harbouring *ssgG* (-459/+679, relative to *ssgG*)	This chapter
pGWS124	pBR-KO with 1.7 kb fragment harbouring the last 228 bp of *ssgE* and the last 1127 bp of SCO3157	This chapter
p*ΔssgC*	Construct for disruption of *S. coelicolor ssgC*	This chapter
p*ΔssgD*	Construct for disruption of *S. coelicolor ssgD*	This chapter
E87/*ΔssgE*	Mutant cosmid with coding region of *S. coelicolor ssgE* replaced by *aac(3)IV*, for gene replacement of *ssgE*	This chapter
8A11/*ΔssgF*	As E87/*ΔssgE*, but for *S. coelicolor ssgF*	This chapter
E19A/*ΔssgG*	As E87/*ΔssgE*, but for *S. coelicolor ssgG*	This chapter

General cloning vectors

pIJ2925 (Janssen and Bibb, 1993) is a pUC19-derived plasmid used for routine subcloning. pBR-KO is a PBR322-based vector for gene disruption in streptomycetes, which has the *Eco*RI-*Hin*dIII section replaced by the multiple cloning site of pUC18, and *tsr* ($Thio^R$) inserted into the *Bam*HI site (Keijser *et al.*, 2003). For cloning in *Streptomyces* we used the shuttle vector pHJL401 (Larson and Hershberger, 1986), which has the pUC19 *ori* for maintenance in *E. coli* and SCP2* *ori* (around 5 copies per chromosome) for maintenance in *S. coelicolor*.

Constructs for the deletion of ssgA-*like genes*

For the creation of vectors for the gene replacement of *ssgC*, *ssgD*, *ssgE*, *ssgF*, and *ssgG*, different strategies were deployed, all resulting in gene replacement constructs where (part of) the coding regions were replaced by the apramycin resistance cassette *aac(3)IV* (Blondelet-Rouault *et al.*, 1997). The coding sequences of the respective genes that were replaced by *aac(3)IV* were: -5/+102 for *ssgC*, +57/+270 for *ssgD*, and the entire coding regions of *ssgE*, *ssgF*, and *ssgG*. For details on the disruption constructs, for constructs for the complementation of the SALP mutants and for the creation of the SALP mutants, see Supplementary Materials and Methods (Noens *et al*,. 2005).

RNA isolation and DNA microarray analysis

S. coelicolor MT1110, an SCP1$^-$, SCP2$^-$ derivative of the wild type prototrophic strain 1147, was grown on Oxoid Nutrient Agar plates (Kieser et al., 2000) and mycelia were collected at 16, 18, 20, 21, 22, 23, 24, 25, 39 and 67 hours after inoculation. The time course sampling was repeated with a new set of cultures for biological replication. Biomass accumulation occurred with two clearly distinguishable phases of logarithmic growth, interceded by a short period (corresponding to sample 4, 21 h after inoculation) marking the transition from vegetative (samples 1-4) to aerial growth (samples 4-8). Spores had already been produced at 39 h, coinciding with growth cessation, and corresponded to the last two time points (samples 9 & 10, 39 h and 67 h after inoculation). For each time point RNA stabilisation, extraction and purification was carried out by methods described at http://www.surrey.ac.uk/SBMS/Fgenomics/Microarrays. For microarray hybridisation each RNA sample was reverse transcribed into Cy3-dCTP-labelled cDNA and co-hybridised with Cy5-dCTP-labelled genomic DNA from *S. coelicolor* M145, as common reference, on *S. coelicolor* M145 PCR-based microarrays. The data from the two biological replicates were averaged. Signal intensities were detected with an Affymetrix 428 laser scanner.

Computer analysis.

The 16-bit TIFF microarray images were analysed with BlueFuse (BlueGnome) spot quantification software and the generated raw data files were imported into GeneSpring^{TM} (Agilent Technologies) for normalisation and analysis of gene expression profiles. Data were normalised per spot (ratio of cDNA to genomic DNA signals) and per chip (ratios divided by the 50th percentile of the ratios within the array). Only data that scored a spot quality

confidence value >0.30 (a parameter calculated by the BlueFuse software) were included in the gene expression analysis. Expression profiles were analysed by hierarchical clustering using the Spearman correlation, which clustered the genes based on profile similarity regardless of their relative expression levels.

The TMPred program (http://www.ch.embnet.org/software/TMPRED_form.html) was used for the prediction of transmembrane domains in proteins and Clustal (Higgins et al., 1996) for multiple protein alignment and for the creation of the phylogenetic tree. Adobe Photoshop^{TM} was used for management of all microscopy images.

Microscopy

Electron microscopy

Morphological studies of surface-grown aerial hyphae and spores of *S. coelicolor* M145 and mutant derivatives by cryo-scanning electron microscopy (cryo-SEM) was performed as described previously, using a JEOL JSM6700F scanning electron microscope (Keijser *et al.*, 2003). Transmission electron microscopy (TEM) for the analysis of cross-sections of hyphae and spores was performed with a Philips EM410 transmission electron microscope as described previously (van Wezel *et al.*, 2000),

Confocal fluorescence microscopy

Impression preparations from the surface of 6-day-old colonies on SFM plates were taken and fixed with methanol. For staining of the DNA, the coverslips were incubated with propidium iodide (1µg ml^{-1}) (Sigma) in the dark for 15 min at room temperature, allowed to air dry and positioned on a microscope slide containing a drop of 20% glycerol, mycelium facing downwards. Staining of the cell wall was performed in 25mM borate buffer pH8, 0.9% sodium chloride + 2mg ml^{-1} BSA, 5µl ml^{-1} FITC-wheat germ agglutinin (Biomedica) for 15 min in the dark at room temperature, allowed to air dry and positioned in a drop of 20% glycerol on a microscope slide. Samples were analysed with a Leica TCS-SP2 confocal fluorescence microscope, equipped with an oil-immersed 100 × Planapo objective and a CCD camera. Digital images were assembled using ADOBE PhotoShop software.

RESULTS

Phylogenetic analysis of SALPs

The *ssgA*-like genes have so far only been identified in actinomycetes that undergo extensive morphological development, and predominantly in streptomycetes. We identified a homologue of *ssgB* in the partial genome sequences of the actinomycetes *Thermobifido fusca* and *Kineococcus radiotolerans*, but it is absent from *Mycobacterium*, *Corynebacterium, Nocardia* and *Rhodococcus*. The streptomycetes whose genome sequence has been completed (*S. coelicolor* and *S. avermitilis*) or almost completed (*S. scabies*) contain six or seven *ssgA*-like genes, and on the basis of hybridization and genomics data we ascertained that *S.lividans* contains the same 7 SALPs as *S. coelicolor* (*i.e.* SsgA-G). Phylogenetic analysis of all known SALP protein sequences revealed three main branches, namely the SsgA branch, the SsgBG branch and the SsgDE branch (Fig. 1). SsgC and SsgF of *S. coelicolor* do not cluster with any of the other proteins, thus forming separate branches, and we have so far only identified homologues of these proteins in *S. lividans*. Analysis of a zoo blot of various streptomycetes (*S. albus, S. fradiae, S. lividans* 1326, *S. coelicolor, S. griseus, S. ramocissimus, S. mobarense, S. cinnamoneus*) revealed homologues of SsgA, SsgB, SsgD, SsgE in all streptomyces species analysed, and typically also SsgG (though absent from *S. avermitilis*), suggesting they constitute the core set of SALPs, which is supplemented by 2-3 additional proteins in probably all streptomycetes.

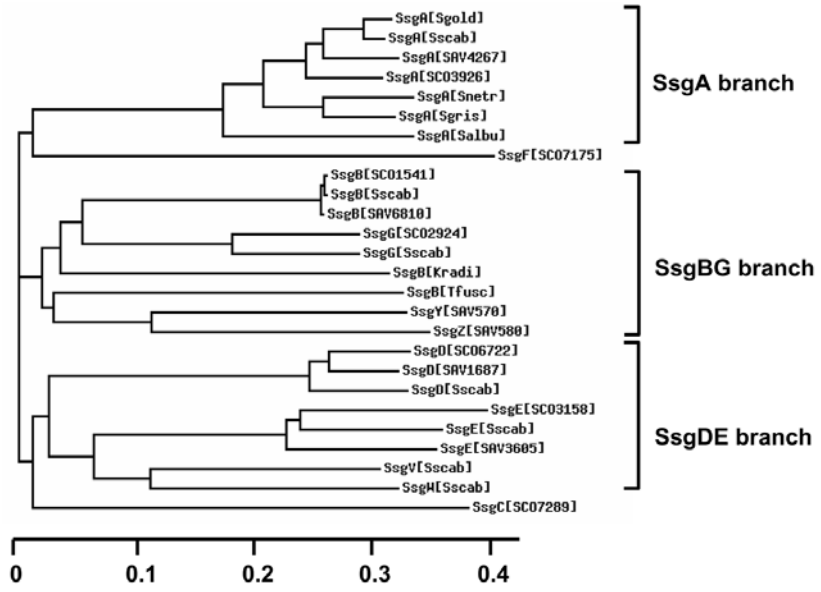

Figure 1: Phylogeny of the SALP protein family. Phylogenetic tree analysis of SsgA-like proteins (SALPs) was done using the ClustalX program. All proteins shown in the figure are listed in Noens *et al.,* 2005, Table S2.

Construction of mutants

The genomic organisation around *ssgC* (SCO7289), *ssgD* (SCO6722), *ssgE* (SCO3158), *ssgF* (SCO7175) and *ssgG* (SCO2924) is shown in Fig. 2. Considering that the genes located downstream of *ssgC*-*ssgG* are divergently transcribed, polar effects due to insertional gene replacements were not anticipated. The individual mutants for each of these genes were created using targeted gene replacement strategies, which are detailed in the Supplementary Materials and Methods (Noens *et al*., 2005). For all individual mutants multiple independent recombinants were obtained, and the correct recombination event was verified by PCR and Southern hybridisation (data not shown). The exact sections of the genes that were replaced by the apramycin resistance cassette *aac(3)IV* were (relative to the translational start): -5/+102 of *ssgC*, +57/+270 of *ssgD*, and precisely the coding regions of *ssgE*, *ssgF* and *ssgG* genes. Since *ssgE* partially overlaps the divergently transcribed ORF SCO3157, which encodes a putative penicillin-binding protein, the latter ORF was restored by integration of plasmid pGWS124, resulting in a wild type SCO3157, but still mutant *ssgE*. This mutant, called GSE1*, was studied alongside GSE1 to ensure that the *ssgE* mutant phenotype was solely due to the replacement of *ssgE* itself and not (entirely or partly) to the disruption of SCO3157. All mutants were restored to the phenotype of the parental strain by the introduction of a low copy-number vector harbouring the relevant *ssgA*-like gene and its promoter sequences. In all experiments described in this paper, we simultaneously analysed the mutants and their genetically complemented derivatives, to verify that all observed abnormalities were due solely to the gene replacement and not to a second-site mutation.

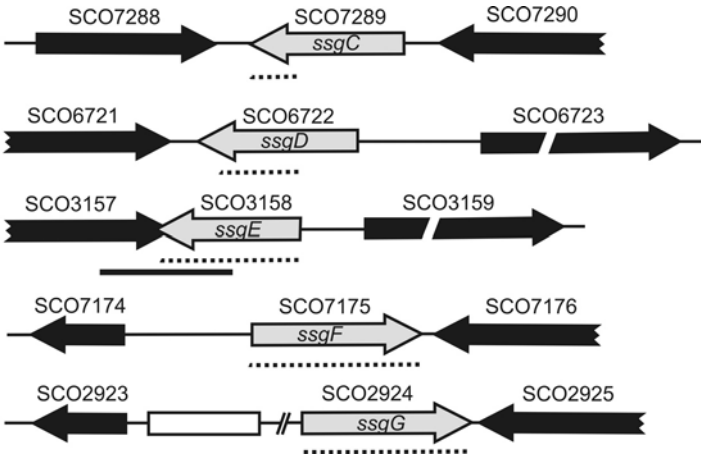

Figure 2: Genetic organisation of the *ssgA*-like genes. *ssgA*-like genes are shown as grey arrows while adjacent genes are shown as black arrows. Above the gene arrows are the corresponding SCO numbers. The dotted line under the *ssgA*-like genes represents (part of) the sequence which is replaced by the apramycine resistance cassette *aac(3)IV* in the knock out mutants. The fragment used for restoration of SCO3157 in the *ssgE* mutant is shown by a bold line.

Phenotypes of the mutants

All seven individual SALP mutants of *S. coelicolor* were plated on various media together with the parental strain M145 (Fig. 3). Sporulation was then assessed visually (spores are grey-pigmented), and verified by phase contrast microscopy and viable counts. The *ssgA* mutant GSA3 had a non-sporulating (White) phenotype on glucose-containing media, while it produced a small amount of spores on the mannitol-containing medium SFM (Fig. 3), in accordance with our earlier observations (van Wezel *et al.*, 2000). The *ssgB* mutant GSB1 displayed the typical unconditional non-sporulating phenotype (Fig. 3) (Keijser *et al.*, 2003).

The new SALP mutants Δ*ssgC-G* all produced grey-pigmented spores after 6 days, although *ssgG* - which is phylogenetically related to *ssgB* - produced significantly fewer spores, highlighted by its light grey appearance (Fig. 3). SsgG belongs to the SsgBG branch of the phylogenetic tree, and both proteins are important for the early stages of septum formation (Keijser *et al.*, 2003) and below). Both the *ssgE* mutant and *ssgF* mutant hyper-sporulated on mannitol-containing media, while there was no significant difference on glucose-containing media (data not shown). Analysis of impression prints by phase contrast microscopy showed that both mutants produced short spore chains, consisting of mostly three or four spores in the *ssgF* mutant, while predominantly single spores where observed for *ssgE* mutant.

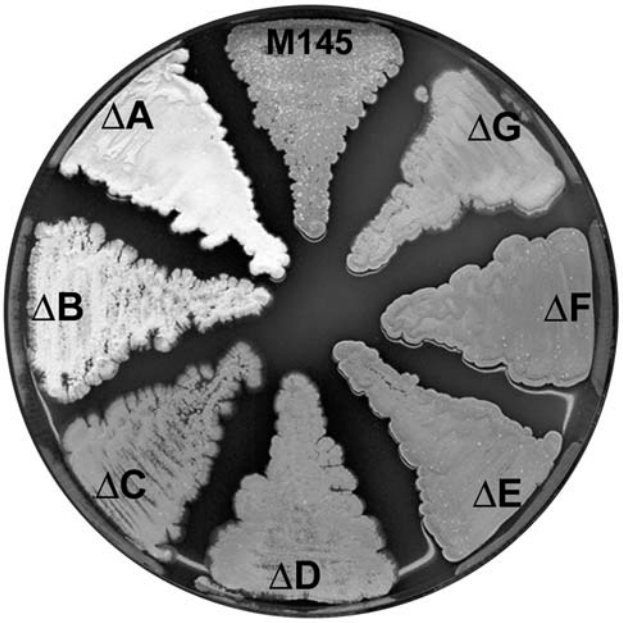

Figure 3: Phenotypes of the *ssgC-G* mutants and their congenic parent *S. coelicolor* M145 on solid media. Strains were grown on SFM at 30°C for 6 days. ΔA, ΔB, ΔC, ΔD, ΔE, ΔF and ΔG are the *ssgA, ssgB, ssgC, ssgD, ssgE, ssgF* and *ssgG* mutants of M145, respectively.

Light microscopy indicated that significant differences in the degree of sporulation also occurred between the *ssgC-ssgF* mutants, verified by repeated spore analyses. Spores were prepared, and diluted to the same spectrophotometric density. Total counts were then done using a haemocytometer and viable counts by plating dilutions (1-10^4 spores/plate) on SFM agar plates. There was a good correlation between microscopic and viable counts, with increased sporulation of GSE1 and GSF1, and reduced sporulation of GSG1. However, spore preparations from the *ssgD* mutant GSD1 consistently contained at least an order of magnitude fewer spores than expected on the basis of its pigmentation, as judged by viable counts and microscopy, suggesting that production of the WhiE spore pigment (Kelemen *et al.*, 1998) was enhanced in this mutant.

Analysis of the mutants by cryo-scanning electron microscopy (cryo-SEM)

Surface-grown colonies of *S. coelicolor ssgC-G* mutants and the parental strain M145 were analysed in detail by cryo-SEM (Fig. 4). *S. coelicolor* M145 produced long spore chains with spore septa at regular intervals, producing 0.8 μm long spores (Fig. 4A-B). Aerial hyphae of the *ssgC* mutant produced extraordinarily long spore chains (Fig. 4C), and contained spores of highly variable lengths (Fig. 4D). In some of the large spores, indentations were visible at the midcell position, suggesting initiated but unfinished septation (Fig. 4D, insert). The *ssgD* mutant produced many straight and undifferentiated aerial hyphae, while spores appeared relatively normal (Fig. 4E-F). Consistent with light microscopy (above), GSE1 and GSF1 sporulated abundantly. The *ssgE* mutant GSE1 showed large areas with only free spores, suggesting premature autolysis-driven spore separation. Perhaps as a result of this spore maturation defect, many of the spores had aberrant sizes in length and occasionally in width (Fig. 4G-H). GSF1 also produced spores of variable sizes (Fig. 4I-J). Cryo SEM failed to visualise the short spore chains typical of the *ssgF* mutant and confirmed by phase contrast microscopy and confocal FM (below); this is most likely a combination of the cryo fixation procedure, where short spore chains are easily lost, and the fact that longer hyphae obscure the shorter ones. *ssgG* mutant GSG1 produced clearly fewer spore chains with normal overall lengths (Fig. 4K), but always containing many irregularly sized spores, most of which were exactly two, three or four times the normal size (detailed in Fig. 4L). As discussed below, septa seem to be occasionally 'skipped' in the *ssgG* mutant.

Confocal Fluorescence Microscopy

Confocal fluorescence microscopy was used to visualise nucleoid distribution and active peptidoglycan synthesis and breakdown during sporulation-specific cell division (Fig. 5, for a full colour version, see p172-173). Nucleic acids were stained with the fluorescent dye propidium iodide (PI), and confirmed using the alternative fluorescent dyes DAPI and 7-aminoactinomycin D (7-AAD). Accumulation of peptidoglycan precursors (as a result of active PG synthesis or breakdown) was visualised by staining with the fluorescein-labelled lectin wheat germ agglutinin (WGA). WGA binds to short oligomers of N-acetylglucosamine (NAG) and N-acetylmuramic acid (NAM), which are alternately coupled to form the peptidoglycan strands (reviewed in (Holtje, 1998)). Fully polymerised peptidoglycan (PG), such as in the mature spore wall, is not recognized by WGA.

The wild type sporulation process on surface-grown cultures is visualised in Fig. 5A, showing fully developed 6 days old *S. coelicolor* M145. Mature spore chains (spo) are not stained with fluo-WGA (right panel), but DNA staining (PI) visualises the completed segregation and condensation of chromosomes (middle panel). In contrast, actively dividing aerial hyphae (aer) are stained very well with fluo-WGA, clearly visualising the build-up of individual septa in a ladder-like fashion, highly similar to FtsZ ladders (Schwedock *et al.*, 1997). Perhaps surprisingly, the DNA still appeared evenly distributed in the aerial hypha, a sign that (completion of) DNA segregation follows septal peptidoglycan synthesis. Earlier stages of sporulation were studied using younger plates (2-4 days old; light image in Fig. 5B, left). WGA binding to the outer side of in particular the spore poles revealed NAM-NAG oligomers, most likely due to peptidoglycan degradation; this shows that these spores undergo the final step of spore maturation, namely the autolytic separation of the cell wall separating the spores (Fig. 5B, right + insert). Expectedly, when wild type spores had fully matured, no WGA staining was observed. DNA had already fully segregated at this stage (Fig. 5B, middle).

The *ssgA* and *ssgB* mutants have a phenotype typical of early sporulation mutants, and fail to produce septa in the aerial hyphae, while vegetative septation was not significantly affected (Keijser *et al.*, 2003; van Wezel *et al.*, 2000). In contrast, the *ssgC* mutant showed extensive *de novo* septum formation in younger aerial hyphae (WGA staining). Surprisingly, coordination of septum formation and DNA segregation was lost in over half of all aerial hyphae seen in this mutant; many empty prespore compartments were observed (Fig. 5D, small arrows), while the intense PI-stained foci indicated the presence of multiple copies of

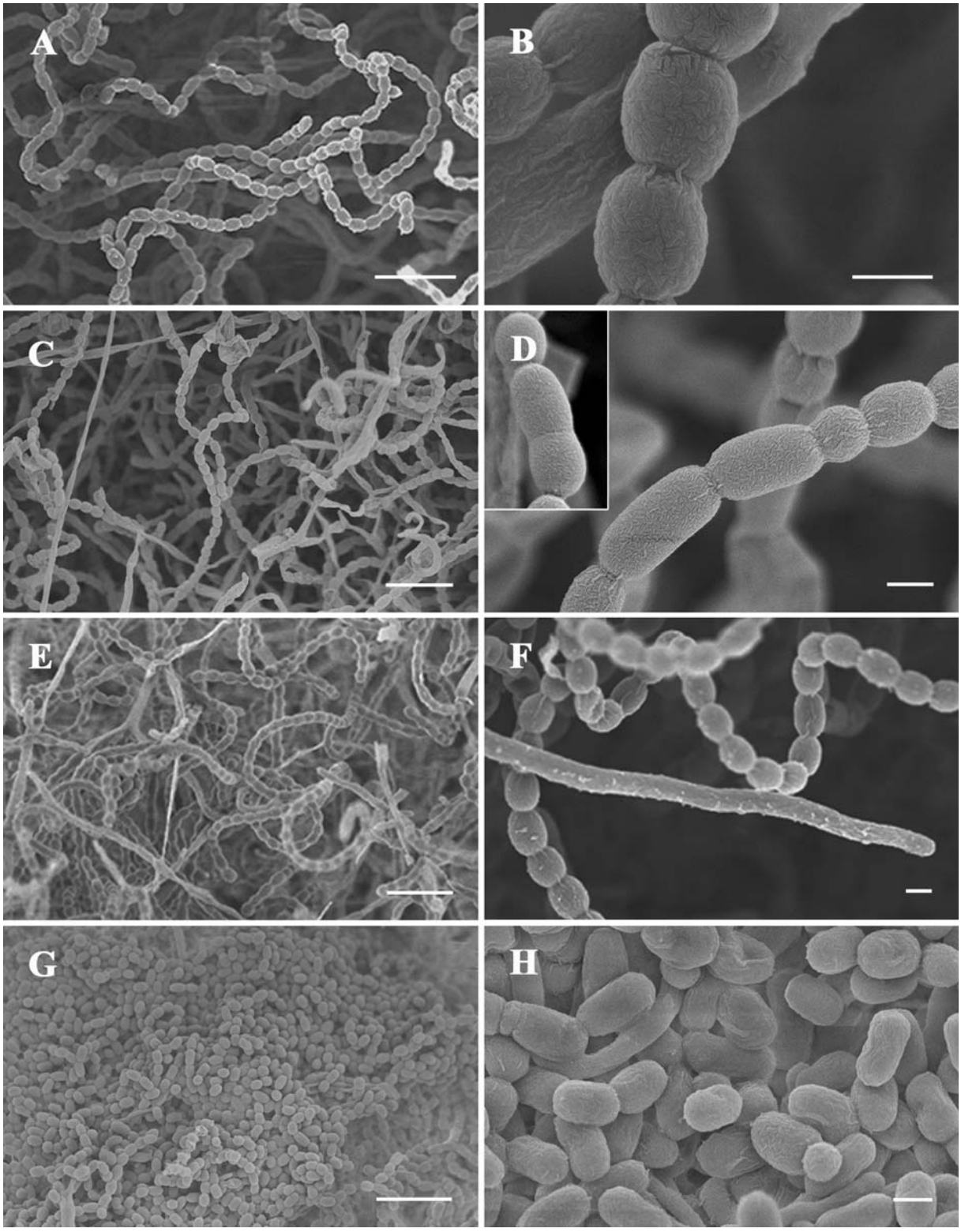
A
B
C
D
E
F
G
H

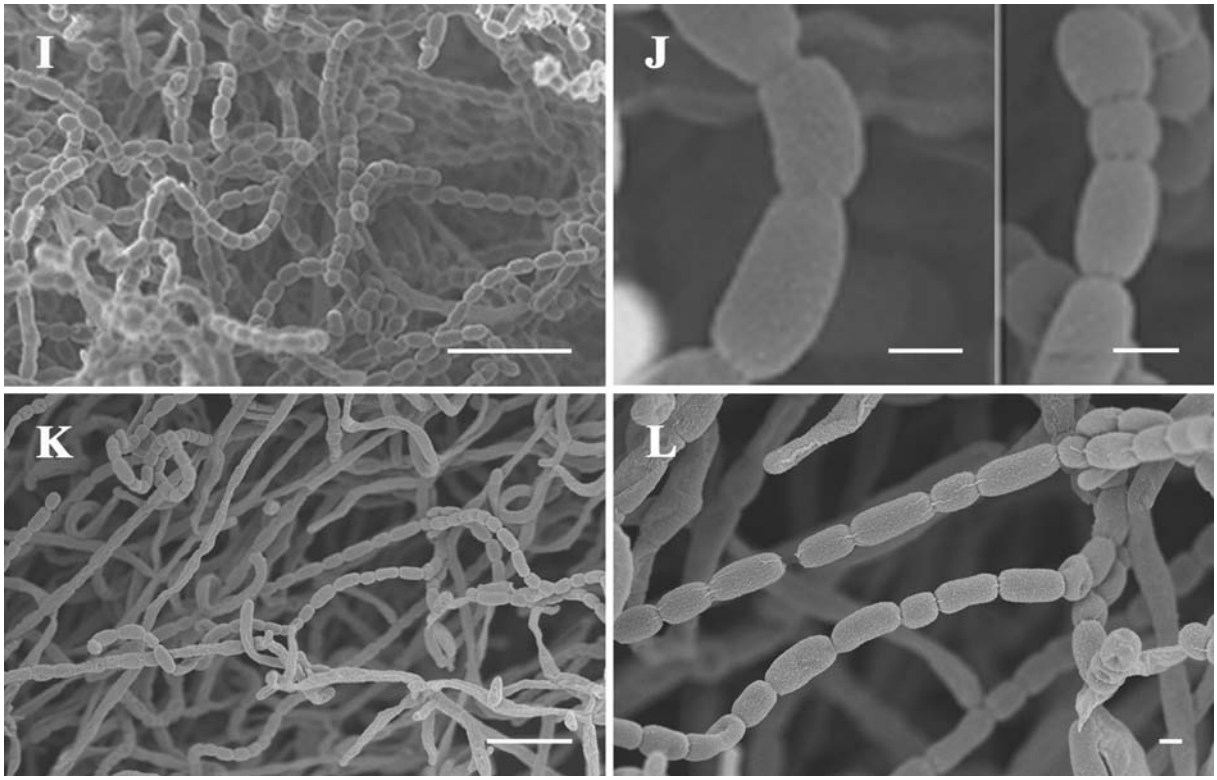

Figure 4: Phenotypic characterisation by cryo-scanning electron microscopy. Samples were taken from 6-day old cultures grown on SFM at 30°C. The left panel shows low magnification (Bar = 5 µm), and the right panel high magnification scanning electron micrographs (Bar = 0.5 µm). **(A-B)** Wild type spore chains of the parental strain M145; **(C-D)** The *ssgC* mutant produces long spore chains **(C)** with spores of irregular sizes **(D)**; **(E-F)** The *ssgD* mutant produced many non-sporulating aerial hyphae and spore chains with irregular spores; **(G-H)** deletion of *ssgE* resulted in the formation of predominantly single spores; **(I-J)** Abundant sporulation of the *ssgF* mutant consisting of spore chains with aberrant spore sizes **(J, insert)**; **(K-L)** *ssgG* mutant with normal- and double-sized spores.

the genome in others (Fig 5D, arrowheads). This is clearly visualised in the DNA/fluo-WGA overlay (Fig. 5D, right panel). Occasionally, spore chains with normal DNA distribution were observed, but these invariably contained mature spores with aberrant sizes (and typically double-sized; Fig. 5C). Spores of the *ssgD* mutant occasionally showed irregular sizes, although DNA distribution appeared normal (Fig. 5E). As described above, mutation of *ssgE* or *ssgF* resulted in strains that sporulated very well, but produced predominantly single spores (*ssgE*; Fig. 5F) or short spore chains (*ssgF*; Fig. 5G). DNA had segregated normally, as shown by the regular pattern of PI staining (middle panels). In contrast to M145, after 7 days of incubation both late sporulation mutants still had many immature spores, and NAG-NAM oligomers were readily identified by WGA staining. In the case of the *ssgE* mutant, only chains of spores were visualised by WGA, and at intersections between adjacent spores. Intriguingly, a large proportion of the *ssgF* spores contained WGA-stained foci exclusively at

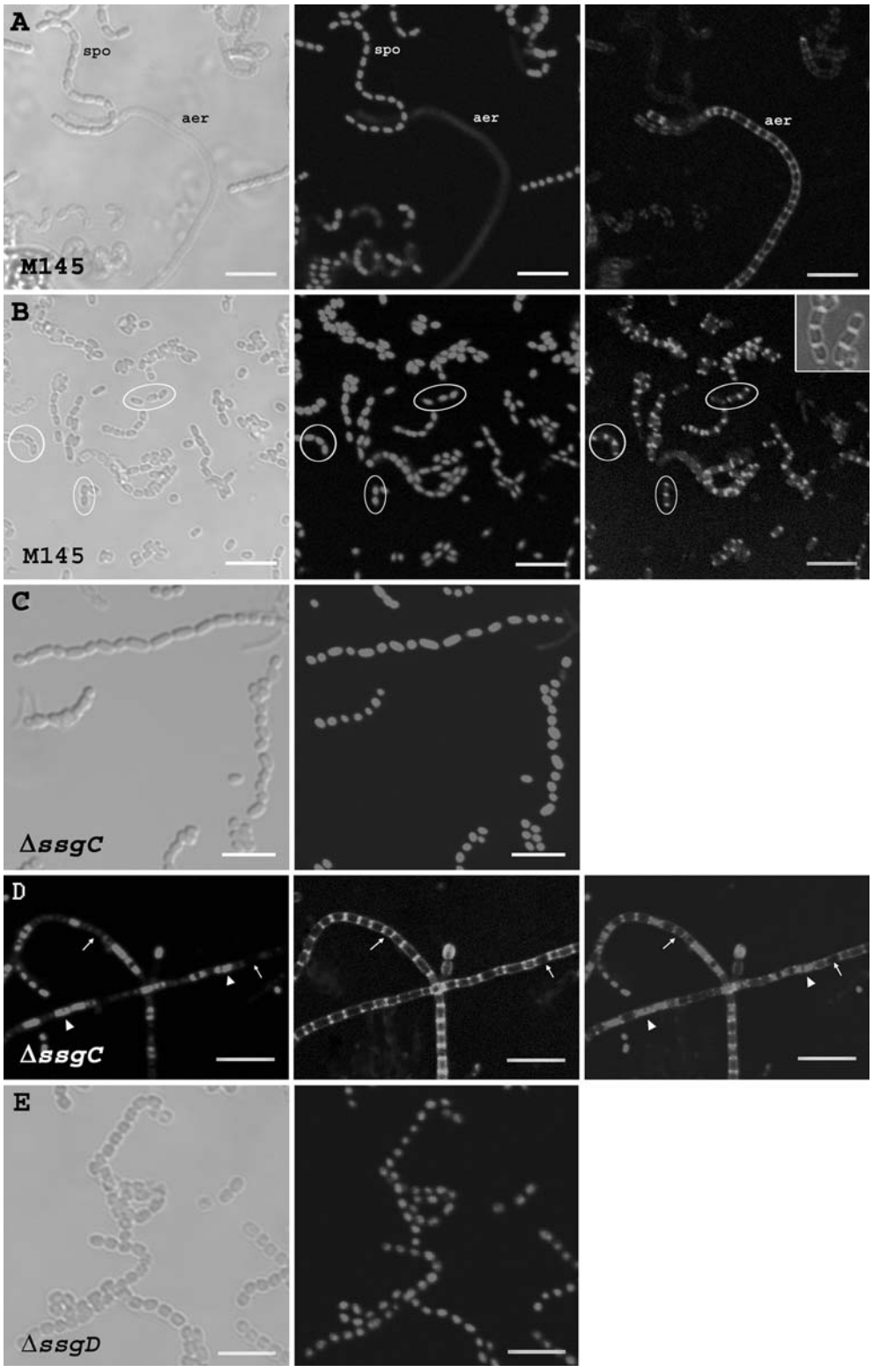
A
spo
aer
M145
spo
aer
aer
B
M145
C
ΔssgC
D
ΔssgC
E
ΔssgD

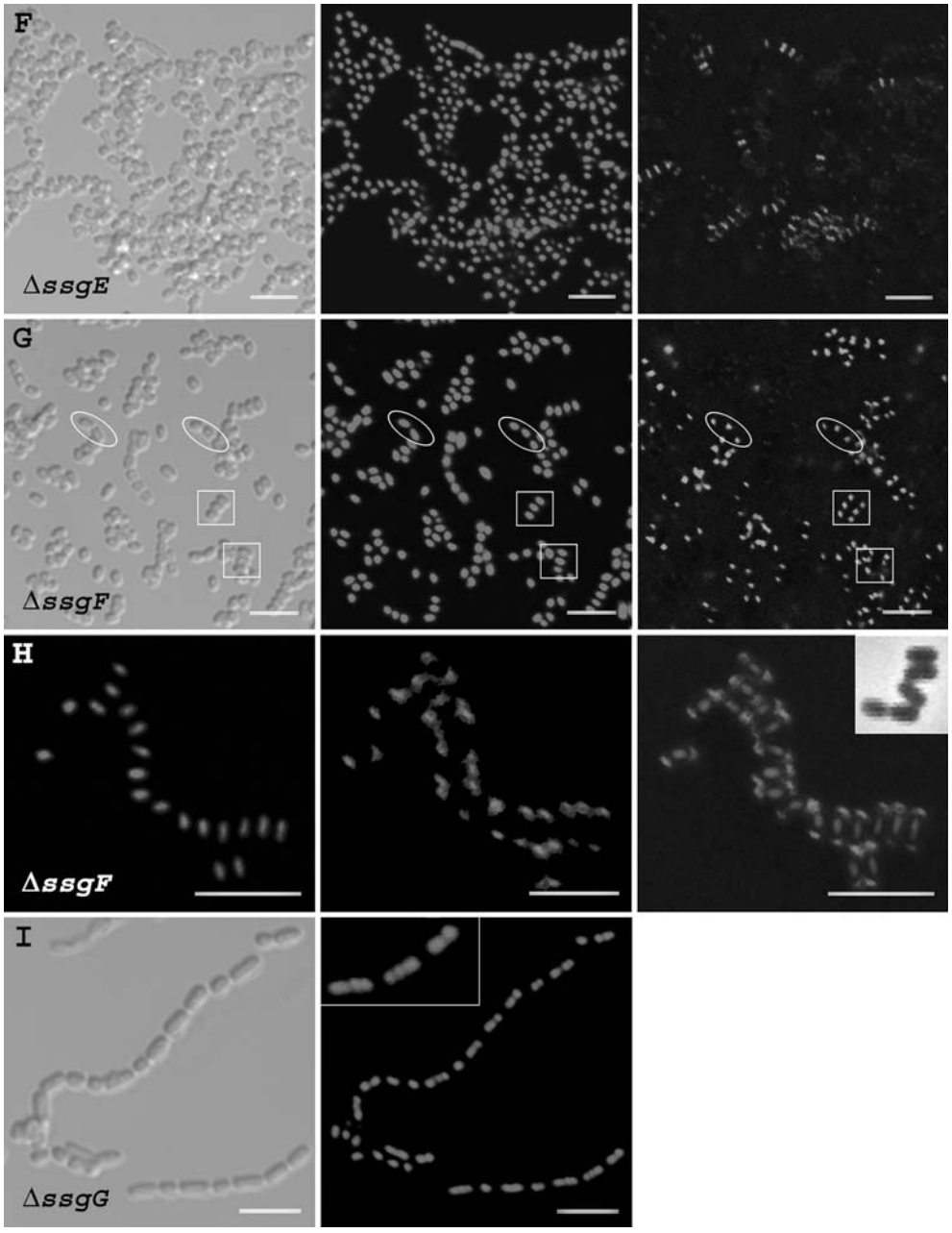

Figure 5: Analysis of the *ssgC-G* mutants by confocal fluorescence microscopy.
Samples were prepared from surface-grown cultures of the parental strain *S. coelicolor* M145 **(A)** and its mutant derivatives Δ*ssgC* **(C-D)**, Δ*ssgD* **(E)**, Δ*ssgE* **(F)**, Δ*ssgF* **(G-H)**, and Δ*ssgG* **(I)** all grown on SFM plates for 6 days at 30°C. *S. coelicolor* M145 **(B)** was grown on SFM plates for 2-4 days at 30°C. DNA and peptidoglycan subunits were visualised with PI (red) and fluorescein-WGA (green), respectively. The first column shows light microscopy micrographs, the middle column shows DNA, and the third column shows peptidoglycan subunits **(A-C, E-G, I)** or the first column shows DNA, the second shows peptidoglycan subunits and the third shows an overlay of PI and WGA **(D-H)**. **(B, insert)** overlay of fluo-WGA and light microscopy of spores of M145 after 2-4 days of growth, clearly showing staining of spore poles by WGA. **(H, insert)** shows a light microscopy micrograph of Δ*ssgF* spores. **(I, insert)** shows a higher magnification of Δ*ssgG* spores with four and respectively three copies of the chromosome. For mature *ssgD* and *ssgG* mutants no WGA stained septa were detected, and images were therefore omitted. Arrowheads show compartments with multiple chromosomes, small arrows show compartments without DNA, white circles highlight WGA-stained spore poles and squares highlight 'rotated' spores. Bar = 5 μm. (Full colour version, see p172-173).

the poles, and always at the outside of the spore walls, similar to M145 in an early stage of the sporulation process (around 4 days old; Fig. 5G). In contrast to the parental M145, where such polar staining disappeared when spores matured, the spores of the *ssgF* mutant always showed this typical polar WGA staining, suggesting a distinct defect in the final stages of autolytic spores separation. Furthermore, many spore chains contained spores that were rotated by 90^0 (Fig. 5G, squares). While such 'rotated' spores were never observed in M145, they constituted approximately 14% (28 out of 201) of all *ssgF* mutant spores. In fact, many spore chains showed a clear transition from normally oriented to rotated spores (Fig. 5H + insert).

As was already apparent from the SEM micrographs, mutation of *ssgG* resulted in many larger compartments with twice, three times or sometimes four times the regular spore size (Fig. 5I + insert). DNA staining clearly identified multiple copies of well-segregated chromosomes in these larger compartments (Fig. 5I), with the DNA content proportional to the increase in spore size (two genomes in a double-sized spore *etcetera*). Thus, DNA segregation could be completed in the absence of septum synthesis (see Discussion).

Transmission electron microscopy (TEM)

TEM was used to closely examine hyphae, septa and spores (Fig. 6). *S. coelicolor* M145 showed typical vegetative cross-walls (Fig. 6A); aerial hyphae produced typical chains of immature (6B) and fully developed mature spores (6C). The spore chains were surrounded by a sheath (small arrow in Fig. 6B-C) that most likely represents the remnants of the parental hyphal wall containing the rodlet layer (David Hopwood, pers. comm.).

The *ssgA* and *ssgB* mutants were studied previously; on mannitol-containing media, the *ssgA* mutant produced occasional regular spore chains (van Wezel *et al.*, 2000), while the *ssgB* mutant was completely devoid of any septa in the sporulation stage (Keijser *et al.*, 2003). Both strains had normal vegetative septa. Interestingly, the *ssgC* mutant strongly resembled the *ssgA*-overexpressing strain GSA3. Around 60% of all cross-walls were irregular (insert in Fig. 6D), as counted from many TEM micrographs of biologically independent samples. In often occurring aberrant vegetative hyphae of the *ssgC* mutant, unfinished cross-walls were observed, which appear like spots of PG in these TEM cross-sections, but are most likely small septal rings in 4D. The distance between them was on average 2 μm (Fig. 6D). The spores of GSC1 were also heteromorphous, with varying lengths and spore walls (Fig. 6E). Interestingly, the *ssgC* mutant strongly fragments in submerged

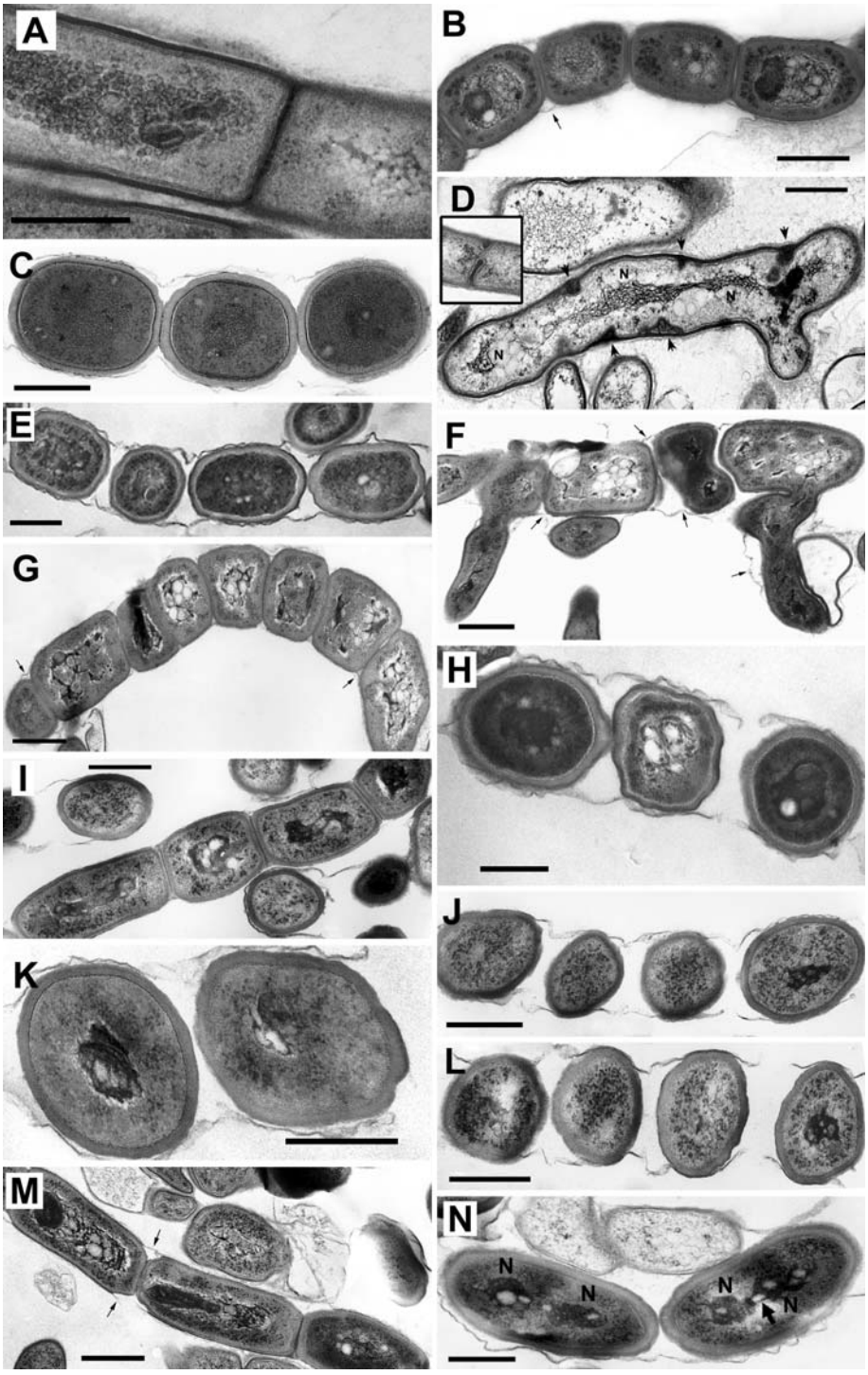

Figure 6: Transmission electron micrographs of hyphae and spores of *S. coelicolor* and its SALP mutant derivatives.
Samples were taken after growth for 6 days on SFM at 30°C. The parental strain M145 produced normal vegetative hypha with cross-walls **(A)**, immature spores **(B)** and mature spore chains **(C)**; In contrast, *ssgC* mutant GSC1 formed irregular vegetative cross-walls **(D+insert)** and heteromorphous spore chains **(E)**. The *ssgD* mutant regularly produced spores with walls with the same width as the aerial hyphae **(F)**, as well as irregular immature **(G)** and mature spore chains **(H)**. Deletion of the late sporulation gene *ssgE* resulted in almost completely normal prespore chains **(I)** and mature spores **(J)**. A large proportion of the mature spore chains of the *ssgF* mutant had spores rotated by 90° **(K-L)**. Around 50% of all spores produced by the *ssgG* mutant were twice, three times or even four times the length of normal spores **(M-N)**, and contained multiple genomes; clearly visible is that the chromosomes had almost completely segregated, but were still linked by a filamentous structure (arrow). The nuclear region is represented by N. Small arrows highlight the sheath surrounding the spore chains. Bar = 0.5 µm.

cultures, and over-expression of *ssgC* inhibits sporulation, again in line with an opposite role of *ssgC* as compared to *ssgA* (not shown).

The *ssgD* mutant showed pleiotropic defects in the integrity of hyphae and spores, perhaps reflecting its high and life-cycle-independent expression ((Traag *et al.*, 2004) and microarray data). Many of the spores had a cell wall similar to that of the lateral wall of non-sporulating aerial hyphae, lacking the typical thick peptidoglycan layer (Fig. 6F). Furthermore, immature spore chains (Fig. 6G) had a highly irregular appearance, with a squashed appearance and with variable spore sizes. Mature spore chains often showed a mix of relatively normal and aberrant spores (Fig. 6H). Analysis of spore preps of GSD1 revealed no difference in heat or lysozyme tolerance to spores from the parental M145 (not shown).

Like most SALP mutants, the *ssgE* mutant produced spores with variable spore sizes (Fig. 6I; see also Fig. 4H). Occasionally, mature spore chains (surrounded by a sheath) were observed but there consistently was a large void between the individual spores.

The *ssgF* mutant produces chains consisting of regular looking spores containing a typical thick spore wall. However, TEM also identified spore chains with spores rotated by 90 degrees, such as also seen by confocal FM (see Fig. 5G-H); here, the individual spores were not attached to each other in the normal head-to-tail fashion, *i.e.* with their spore poles adjacent to each other, but rather in a parallel fashion, resulting in a wider spore chain (800 nm instead of the regular 600 nm; Fig 6K-L).

As SEM and FM analysis of the *ssgG* mutant, also TEM revealed many large spores, with exactly twice, three times or even four time the normal length (Fig. 6M). TEM clearly confirms the presence of multiple genomes in the larger spores, while there is no evidence of any cell wall material between the almost completely segregated chromosomes. This shows that septal peptidoglycan synthesis and DNA segregation are uncoupled in this mutant. Interestingly, while the chromosomes are almost completely separated, they are still attached to each other through a thin filamentous structure (Fig. 6N, arrow).

DNA microarray analysis of cell division and developmental genes

The data above established that the SALPs play a role in the control of peptidoglycan synthesis and autolysis. To judge which PBPs and autolysins present on the *S. coelicolor* genome are most obvious candidates for peptidoglycan synthesis during development, and relate functionally to SALPs, we performed microarray analyses on *S. coelicolor* (Fig. 7, p176). Transcription of SALP genes was compared to that of genes involved in the

maintenance of the peptidoglycan (PBPs and autolysins). As for the SALP genes, microarray analysis of *ssgA* and *ssgC* produced data below the confidence threshold. Detailed analysis performed previously showed that transcription of *ssgA* and its activator *ssgR* is induced towards the onset of sporulation, and *ssgD* is strongly transcribed throughout development (Traag *et al.*, 2004). Microarray data (Fig. 7B, p176) support this for *ssgD* and *ssgR*, and show that *ssgB* is strongly activated towards sporulation. Of the two spore maturation genes, *ssgE* is expressed at a low level, while *ssgF* is strongly expressed, both with a life-cycle independent expression profile. Finally, *ssgG* is expressed relatively strongly during vegetative growth and again towards sporulation, suggesting a possible role in both developmental stages. The expression profiles were confirmed by promoter probing using the *redD* promoter-probe system (van Wezel *et al.,* 2000c). Particularly *ssgB*, *ssgD,* and *ssgF* were expressed in the aerial hyphae (not shown). The transcription profiles were all confirmed by RT PCR analysis and by promoter probing, except for *ssgF*; while microarrays predicted high and almost growth-phase independent expression, detailed analysis showed that *ssgF* is in fact expressed during sporulation, and at a low level.

Several *pbp* genes are developmentally controlled (Fig. 7B, p176). SCO3847 and SCO4013, both encoding homologues of *Bacillus* PBP3, were upregulated during both the onset of both vegetative and aerial growth; SCO5487 and SCO5039 were switched on primarily during early vegetative growth, while the *ftsI*-like genes SCO3156 and SCO3771 were induced at a time related to aerial growth, although transcription of SCO3156 was switched off again during sporulation.

Autolysins are responsible for the breakdown of peptidoglycan, *e.g.* during spore separation. Several autolysins are developmentally controlled; these are either switched on during both vegetative and aerial growth (SCO2116, for one of several AmpD-type autolysins), or relate to a specific developmental stage, namely at a time related to aerial growth (SCO5466, encoding a lysozyme-like autolysin) or to sporulation (SCO4132, encoding the SLT autolysin, the only lytic transglycosylase in *S. coelicolor*). Interestingly, in collaboration with Dr. Rigali (Liege, Belgium) we recently discovered that SCO5466 is strongly downregulated in a *crp* mutant, which fails to produce the cAMP receptor protein CRP (Piette *et al.*, submitted for publication). This mutant is strongly disturbed in autolysis of the prespore chain, confirming the likely involvement of SCO5466 in spore maturation.

DISCUSSION

This paper discusses the role of the SsgA-like proteins in the control of specific aspects of the sporulation process, from initiation of septal peptidoglycan synthesis to the separation of spores from the maturing prespore chain. To better discuss their individual functions, we discriminate between the following landmark events during the sporulation process in aerial hyphae of *Streptomyces* (Fig. 8); (I) Prespore formation, consisting of (IA) septum site selection; (IB) septum initiation; (IC) septum growth; (ID) DNA segregation and condensation; (IE) septum closure; and (II) spore maturation, consisting of (IIA) growth (thickening) of the spore wall peptidoglycan; (IIB) Spore separation by PG autolysis; (IIC) Spore release. Our data show that each of the individual SALP genes affects one of these landmark events, and relate to the control of peptidoglycan synthesis or breakdown. This includes the first examples of proteins that control the exact sites where septa are initiated (stage IA, by SsgG) and autolytic spore separation (stage IIBC, by SsgE and SsgF). The phenotypes of the mutants and the suggested function of the genes during sporulation are summarised in Table 3.

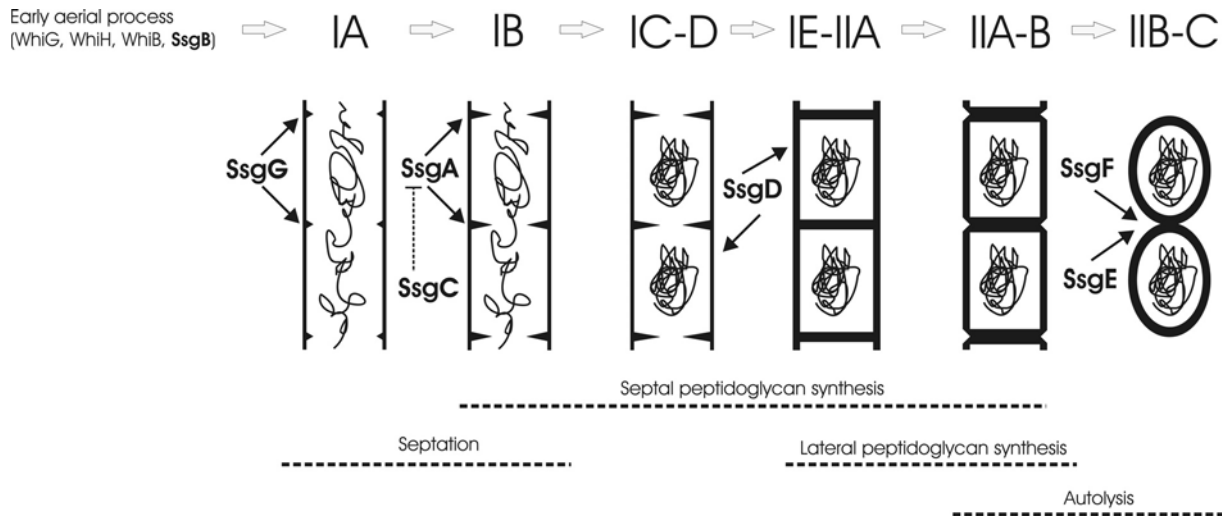

Figure 8: Model of the development of sporulation-committed aerial hyphae and suggested function of SALPs.
Several events observed during the sporulation process in aerial hyphae of *Streptomyces* are shown; (I) Prespore formation, consisting of (IA) septum site selection; (IB) septum initiation; (IC) septum growth; (ID) DNA segregation and condensation; (IE) septum closure; and (II) spore maturation, consisting of (IIA) growth (thickening) of the spore wall peptidoglycan; (IIB) Spore separation by PG autolysis; (IIC) Spore release. The dotted lines represent specific events that occur in the sporulation process. A suggested role for the SALPs is indicated in the figure. SsgB is most likely involved in the signalization for growth cessation. SsgG controles septum site localisation. SsgA is involved in the initiation of septum formation, and is antagonised by SsgC. The function of SsgD is related to the synthesis of peptidoglycan along the lateral cell wall. SsgE and SsgF are involved in the autolysis of the mature spore chain with SsgE controlling correct timing of spore dissociation, and SsgF ensuring correct final stages of autolytic detachment. See Discussion.

Table 3: Phenotype of the SALP mutants and the timing of activity during development.

Gene	Phenotype of SALP mutants	Timing of activity[a]
ssgA	Conditional non-sporulating phenotype; enhanced expression stimulates sporulation-specific cell division	Septum initiation (IB).
ssgB	Strictly non-sporulating phenotype, very large ("immortal") colonies.	Correlates temporally to growth cessation of aerial hyphae prior to onset of sporulation
ssgC	Irregular spores, imperfect segregation of DNA, very long ladders of spore septa.	Controls septum site initiation and DNA segregation (IB)
ssgD	Aberrant spore wall.	Lateral cell wall synthesis (IIA).
ssgE	Predominantly single spores due to accelerated autolysis.	Correct timing of spore dissociation (IIB-C).
ssgF	Short spore chains; old spores were stained with WGA at the outside of the spore poles; rotated spores.	Final stages of spore separation (IIB-C).
ssgG	Septa are regularly skipped, without affecting DNA segregation. Many spores exactly two, three or four times the normal size.	Controls septum site localisation (IA).

a. Numbers (IB-IIC) correspond to developmental phases illustrated in Figure 6.

Control of peptidoglycan synthesis during prespore formation

Microarray data (Fig. 7, p176) and previously published transcriptional analyses revealed that *ssgA* and *ssgB* and to a lesser extent *ssgG* are induced during late aerial growth and early sporulation. Deletion of these genes results in complete (*ssgA*, *ssgB*) or partial (*ssgG*) loss of the ability to sporulate. The aerial hyphae of the *ssgA* and *ssgB* mutants are essentially aseptate. Over-expression of *ssgA* resulted in hyper-septation of both vegetative and aerial hyphae, and TEM micrographs revealed many extremely thick and unfinished cross-walls in the vegetative hyphae, leaving a distinct gap in the middle (van Wezel *et al.*, 2000). This strongly suggests that SsgA activates the initial steps in the polymerisation of septal peptidoglycan. *ssgB* is the most highly conserved cell division-related gene in actinomycetes, and a rare example of a *whi* gene that is not a transcriptional regulator. *ssgB* mutants produce very long aseptate aerial hyphae, forming 'immortal' colonies (Keijser *et al.*, 2003). The sporulation process is initiated as soon as aerial growth ceases (Chater, 2001), requiring a block of PBP2 enzyme activity, and this signal most likely depends on SsgB. Interestingly, many granules accumulate in the hyphae of the *ssgB* mutant (Fig. S3, Noens *et al.*, 2005), which due to their electron-dense nature are likely to contain unincorporated cell wall precursor material. The same granules were also observed in the PBP2 mutant (a kind gift from Dr. G. Hobbs), providing evidence of a functional relationship between SsgB and PBP2.

The function of SsgC is the reverse of that of SsgA. *ssgC* mutants produce the spiral-like distribution of peptidoglycan along the wall of vegetative hyphae, typical of SsgA-overexpressing strains. Also, extraordinary long ladders of septa are often observed in this mutant, with disturbed DNA segregation, similar to strains over-expressing SsgA. *ssgC* is one of the two strain-specific SALPs of *S. coelicolor*. So far, we have only found homologues of

ssgC in strains with low expression of *ssgA* (such as *S. coelicolor* and *S. lividans*; unpublished data). On the basis of our observations, we propose that SsgC functions as an antagonist of SsgA.

The *ssgG* gene is a rare cell division mutant, and an opportunity to improve our understanding of how multiple septum sites are selected and chromosomes are segregated in streptomycetes. Typically, highly regular ladders of septa are produced in sporulation-committed aerial hyphae (Grantcharova *et al.*, 2005; Schwedock *et al.*, 1997). In the *ssgG* mutant, at irregular intervals septa were simply 'missing', resulting in spores exactly twice, three times or even four times the size of normal spores. Excitingly, the chromosomes were well segregated in these multiple-sized spores, resulting in long spores with up to four chromosomes joined only by a thread-like filamentous structure. TEM showed the complete absence of any cell wall material (peptidoglycan) between the segregated chromosomes. So while in wild type cells septal peptidoglycan synthesis is always initated prior to DNA segregation (*e.g.* Fig. 5A), the *ssgG* mutant reveals that in fact the initiation of septal peptidoglycan synthesis is not a requirement *sine qua non* for correct DNA segregation. This sheds new light on this intriguing process.

ssgD mutants produce many prespores and spores with aberrant hyphal walls, including spores with a wall the width of regular hyphae, and irregular prespore chains, suggestive of weakened lateral peptidoglycan. The synthesis of lateral PG is carried out by PBP2 (SCO2605) (Den Blaauwen *et al.*, 2003; Errington *et al.*, 2003) and the highly similar protein encoded by SCO2897. Interestingly, mutational analysis showed that both PBP2 and SCO2897 – revealed by microarray analysis to be strongly expressed throughout the *S. coelicolor* life cycle - are indeed important for lateral wall PG synthesis (G. Hobbs, proceedings of ISBA XIII, Melbourne 2003), suggesting that SsgD allows the correct functioning of at least one of these two PBPs.

Spore maturation: SsgEF control autolytic spore separation

While the insight in the sporulation process in streptomycetes is rapidly improving, little is known of the final stage, the autolytic cleavage of the peptidoglycan connecting the prespores, resulting in mature and separated spores. Our data show that SsgE and SsgF play a specific role in the control of this process. Strains lacking *ssgE* sporulated very well, with normal septation and DNA segregation, but produced predominantly single spores. Since prespores were invariably organised in spore chains, the high frequency of single mature spores must

have arisen from an accelerated maturation process followed by a non-coordinated separation into single spores. This implicates SsgE as a checkpoint for the correct timing of spore dissociation. Interestingly, all streptomycetes whose genome has been sequenced have one SALP that is predicted by the TMPred algorithm to have a transmembrane helix, namely SsgF (aa 14-32) in *S. coelicolor*, SsgW (aa 51-75) in *S. scabies* and SAV580 (aa 85-103) in *S. avermitilis*, with a strong preference for the N-terminus facing the cytoplasm. *ssgF* plays a distinct role during the final stage of spore separation. Deletion of the gene resulted in short spore chains, with spores that were readily stained by WGA, invariably at the poles and at the outside of the spore wall. Since *de novo* synthesis occurs from inside to outside, these peptidoglycan subunits accumulated at the spore poles must have resulted from autolysis of the spore-linking peptidoglycan. Hence, in the absence of SsgF spores fail to complete autolytic detachment due to incomplete breakdown of PG subunits, resulting in more loosely attached prespores and allowing almost free rotation. This is substantiated by our observation of a "flip movement" in several spore chains, with a visible transition from normally oriented spores (poles connected head-to-tail) to 90 degrees rotated spores (poles parallel), with an intermediate spore (45 degrees rotated) in between (Fig. 5H + insert). The likely driving force is the stronger hydrophobic interaction between the long sides of the spores as compared to the poles. Thus, SsgF ensures the final step in autolysis of prespores.

SALPs and the fate of peptidoglycan

Scientists have been searching for an answer to the important question as to how streptomycetes coordinate the synchronous formation of multiple septa and the concomitant segregation of the same number of chromosomes. The cell division machinery is generally very similar to that of other eubacteria, although especially aspects of regulation and localisation are different. Which then are the proteins that make sure that septa are layed down simultaneously, and with such striking regularity? It is likely that this involves *Streptomyces*-specific proteins. The SALPs are obvious candidates; they occur exclusively in actinomycetes that undergo extensive morphological differentiation. Four of the SALPs are present in all streptomycetes, namely *ssgA, ssgB, ssgD,* and *ssgE*, while *ssgG*-type genes are also relatively common. Sequence conservation of the predicted gene products varies from 55% (SsgE) to 100% (SsgB), SsgB being the most highly conserved cell division protein in *Streptomyces* (Flärdh and van Wezel, 2003). Our data now show that all SALPs relate specifically to sporulation-specific cell division, as *ssgX* mutants have various defects in the

build-up or degradation of peptidoglycan during sporulation, but show normal vegetative growth and regular cross-walls. The only exception is the *ssgC* mutant; as discussed, its phenotype is highly similar to a strain over-producing SsgA, showing not only developmental defects, but also the typical enhanced and irregular septation in vegetative hyphae.
The main question that is not so easily answered is what exactly is the mechanism by which the SALPs control the different steps of the sporulation process? At this point, it is important to note that while the classical early *whi* genes such as *whiA,whiB, whiG, whiH, and whiN* (*bldN*) encode (predicted) DNA binding proteins such as σ factors and GntR-family regulators, and hence most likely function at the level of transcriptional control (and are therefore less obvious candidates for an interaction with PBPs and autolysins), ssgA and ssgB are *whi* genes that likely encode structural proteins. Interestingly, we recently obtained convincing evidence that at least SsgA and SsgF form multimers with itself *in vitro* even under denaturing conditions - with up to 5-membered multimers confirmed by mass spectrometry of purified SsgF (GVW, unpublished data). This indicates that SALP multimerisation probably is an essential part of their function. SALPs have no known protein motif, and lack DNA binding activity, which suggests that SALP multimers function by recruiting other proteins to their relevant sites, so as to manage enzymes responsible for the synthesis and autolysis of peptidoglycan.

On the basis of our data we predict the following functional relationships. SsgA - antagonised by SsgC - directly stimulates cell division and the build up of septal PG, and hence it functionally relates to the developmental PBPs involved in septal PG synthesis, *ie.* FtsI, SCO3171 and/or SCO3156. On the basis of the highly similar phenotypes of the respective mutants, PBP2 relates functionally to SsgB, and SCO2897 and/or PBP2 - which are both important for lateral wall PG synthesis - to SsgD. SsgE and SsgF control autolytic spore cleavage, with SsgE preventing premature spore release, a function most likely carried out by SCO5466, and SsgF promoting the cleavage of peptidoglycan strands between the spores in almost mature prespore chains, in prokaryotes carried out by SLT. In accordance with this, SCO5466 and SLT are transcribed in a highly developmental way, suggesting their involvement primarily in spore separation. Finally, SsgG is the first example of a protein specifically involved in the coordination of multiple septation, a unique feature of *Streptomyces* cell division. Solving the question as to how SsgG determines the exact sites

where cell division is initiated will greatly improve our understanding of this intriguing phenomenon.

To further characterise the nature of all functional interactions, we are currently conducting extensive expression analyses in all SALP mutants using genomics approaches, and concentrate on the identification of the exact interaction partners for the SALPs.

ACKNOWLEDGMENTS

We are very grateful to Dr. Glyn Hobbs (Liverpool, UK) for the PBP2 mutant and for discussions, to Hans van der Meulen for excellent technical assistance with TEM, and to Dr. Erik Vijgenboom and Dr. Barend Kraal (Leiden, the Netherlands) and Prof. Sir David Hopwood for discussions. This work was supported by grants from the Netherlands Academy for Arts and Sciences (KNAW) to GPVW and from the BBSRC (UK) to CPS.